

# Crystallization Kinetics of a PEEK/LCP Blend

BENJAMIM DE CARVALHO and ROSARIO E. S. BRETAS

Department of Materials Engineering, Universidade Federal de São Carlos, 13565-905 São Carlos, SP, Brazil

## SYNOPSIS

The crystallization kinetics of a polyetheretherketone (PEEK)/liquid crystalline polymer (LCP) blend was studied by using differential scanning calorimetry. Nonisothermal runnings were performed on heating and on cooling at different rates. Isothermal crystallization experiments at 315, 312, 310, and 307°C, from the melt state (380°C) were performed in order to calculate the Avrami parameters  $n$  and  $k$  and the fold surface free energy,  $\sigma_e$ . Polarized light optical micrographs were also obtained to confirm the Avrami predictions. It was observed that the LCP retarded the PEEK crystallization process and that the PEEK melting temperature decreased with the amount of LCP, but the LCP melting temperature increased with the amount of PEEK. Probably the PEEK improves the perfection of the LCP crystalline domains. A spherulitic morphology in pure PEEK and its blends was predicted by the Avrami analysis; however this morphology was only observed for pure PEEK and for the 80/20 composition. The other compositions presented a droplet and fibrillar-like morphology. The overall crystallization rate was observed to decrease with the crystallization temperature for all compositions. Finally,  $\sigma_e$  was found to decrease with the increase of LCP in the blends, having unrealistic negative values. Thus, calculations were made assuming  $\sigma_e$  constant at all compositions. It was observed that  $\sigma$ , the interfacial lateral free energy, decreased but still remained positive. It was concluded that in these blends neither  $\sigma_e$  nor  $\sigma$  could be considered constant. © 1995 John Wiley & Sons, Inc.

## INTRODUCTION

The crystallization kinetics of a pure polymer has been traditionally studied by using the Avrami analysis, together with crystallization rates measured by polarized light optical microscopy, and the Hoffmann et al. kinetic theory of crystallization with chain folding, with<sup>1,2</sup> and without<sup>3</sup> reptation.

The Avrami approach has numerous disadvantages; however, the  $n$  and  $k$  parameters can be used to interpret qualitatively the nucleation mechanism and morphology and overall crystallization rate of the polymer, respectively. The Hoffmann et al. kinetic theory, on the other hand, allows the calculation of the overall crystallization growth rate of three theoretically defined crystallization regimes, each one ruled by a different nucleation mechanism from the melt.

In binary blends, the analysis is more complex. In the case of compatible blends,<sup>4</sup> for example, it is known that crystallization rates will be different from pure polymer due to a dilution effect; usually a decrease in crystallization rates is observed as the weight fraction of the noncrystallizable polymer increases.<sup>5-7</sup> It has also been observed that the fold surface free energy of the crystallizable polymer,  $\sigma_e$ , is constant at all compositions.<sup>8</sup> The kinetics in partially miscible or immiscible blends has not been extensively studied as in completely miscible blends.

In a recent work,<sup>9,10</sup> the miscibility and crystallization kinetics of polyetherimide (PEI)/polyetheretherketone (PEEK)/liquid crystalline polymer (LCP) ternary blends were reported. It was observed that the cold crystallization temperature of the PEEK/LCP binary blends was constant; however, the cold crystallization temperature of the PEEK/PEI binary blends increased with the amount of PEI. The PEEK/LCP blends were found to be partially miscible before annealing, and the PEEK/PEI blends were miscible before and after the thermal

\* To whom correspondence should be addressed.

treatment. In the ternary blends a similar behavior was observed. However, in this case, the LCP seemed also to affect this temperature in a nonpredictable way. The Avrami parameters changed with the crystallization temperature and composition; compositions with high concentrations of PEI or LCP needed higher times for crystallization to begin and higher times for maximum crystallization to occur. In some of the ternary blends a decrease was also observed in crystallization rates as the amount of PEI increased. Again, the influence of the LCP on the PEEK crystallization was observed, but no definitive conclusions could be obtained because being ternary blends, the PEI also affected the crystallization behavior. Thus, it was verified that in order to clarify this influence, it was necessary to study the crystallization kinetics of binary blends made solely of PEEK and LCP.

The objective of this work was to analyze in what ways the LCP influences the PEEK crystallization mechanism, by using the Avrami and Hoffmann et al. analyses.

## THEORETICAL BACKGROUND

For homopolymers, the Avrami parameters  $n$  and  $k$  can be calculated from the equation<sup>11</sup>:

$$\ln \{ [1 - X_c(t)] / X_\infty \} = -kt^n \quad (1)$$

where  $X_c(t)$  = degree of crystallinity as a function of time and  $X_\infty$  = ultimate crystallinity at very long times.

The calculations are made from data of isothermal crystallization experiments from the melt and/or glass-transition temperature,  $T_m$  and  $T_g$ , respectively.

$\sigma_e$  is related to the free energy of formation of a crystal by the equation:

$$\Delta\phi_{\text{crystal}} = 4xl\sigma + 2x^2\sigma_e - x^2l(\Delta f) \quad (2)$$

where  $\Delta\phi_{\text{crystal}}$  = free energy of formation of a single chain folded crystal;  $l$  = thin dimension of the crystal;  $x$  = large dimension of the crystal;  $\sigma$  = lateral surface interfacial free energy; and  $\Delta f$  = bulk free energy of fusion.

$\sigma_e$  is also related to the overall crystallization rate,  $G$ ,<sup>3,6,7</sup> by the following equation:

$$G = G_0 \exp[-U^*/R(T - T_\infty)] \\ \times \exp[-rb_0\sigma_e/(\Delta f)KT]$$

$$= G_0 \exp[-U^*/R(T - T_\infty)] \\ \times \exp[-K_g/T(\Delta T)f] \quad (3)$$

where  $G_0$  = preexponential factor (independent of the temperature);  $U^*$  = activation energy for reptation in the melt;  $T_\infty$  = theoretical temperature at which reptation ceases;  $b_0$  = thickness of the surface nucleus;  $K$  = Boltzmann constant;  $f = 2T/T_m^\circ + T$ ;  $K_g$  = nucleation constant;  $T_m^\circ$  = equilibrium melting temperature; and  $r$  = parameter characteristic of the growth regime (4 for regimes I and III and 2 for regime II).

From the Avrami approach:

$$k \propto G^n \quad (4)$$

For miscible blends, the noncrystallizable component can be regarded as a diluent, and  $G$  can be calculated by<sup>8</sup>:

$$G = \varphi_2 G_0 \exp\{-U^*/R[C_2 + T - T_g(\varphi)]\} \\ \times \exp\{-rb_0\sigma_e T_m^\circ(\varphi)/[Kf\Delta H_m^\circ T\Delta T(\varphi)]\} \\ \times \exp\{2\sigma T_m^\circ(\varphi)\ln\varphi_2/[b_0f\Delta H_m^\circ\Delta T(\varphi)]\} \quad (5)$$

where  $\varphi_2$  = volume fraction of the crystallizable polymer;  $T_g(\varphi)$  = glass-transition temperature of the blend (composition dependent);  $C_2$  = WLF constant = 51.6°C;  $T_m^\circ(\varphi)$  = equilibrium melting temperature of the crystallizable component (composition dependent);  $\Delta H_m^\circ$  = equilibrium heat of fusion; and  $\Delta T(\varphi) = T_m^\circ(\varphi) - T$  = actual undercooling.

By using eqs. (4) and (5) a final expression for the growth rate can be found<sup>7,8</sup>:

$$A = (\ln k/n) + \{U^*/R[C_2 + T - T_g(\varphi)]\} \\ - [1 + 2\sigma T_m^\circ(\varphi)/b_0f\Delta H_m^\circ\Delta T(\varphi)] \ln \varphi_2 \\ = \ln G_0 - rb_0\sigma_e T_m^\circ(\varphi)/Kf\Delta H_m^\circ T\Delta T(\varphi). \quad (6)$$

Thus the slope of a plot of the left-hand term of eq. (6),  $A$ , as a function of  $1/T\Delta T$  yields  $\sigma_e$ , if  $r$ ,  $b_0$ ,  $\sigma$ ,  $T_m^\circ(\varphi)$ , and  $\Delta H_m^\circ$  are known. To evaluate  $\sigma$ , usually the Thomas–Stavely equation is used<sup>7,8</sup>:

$$\sigma = \beta\Delta H_m^\circ(A_0)^{1/2} \quad (7)$$

where  $\beta = 0.1$  (polyolefins);  $\beta = 0.24$  (for some polyesters); and  $A_0$  = cross-sectional area of the chain in the crystal.

## EXPERIMENTAL

### Materials

The polymers used in this study were a PEEK (Vicatex 450G) from ICI Co. and an LCP (HX4000) from DuPont. The LCP is a polyester based on terephthalic acid, phenylhydroquinone, and hydroquinone.

### Blending

Before blending, the three polymers were vacuum dried at 120°C for 1 day. Each composition was first tumbled in a container on a weight ratio basis, then melt blended, pelletized, and finally injection molded. Melt blending was performed in a Killion extruder (model KL-100) at an average temperature of 370°C. Injection molding was performed in an Arburg injection molding machine (model 221-55-250) using the following barrel temperatures: zone 1, 350°C; zone 2, 380°C; zone 3, 385°C; zone 4, 390°C. The mold was held at 112°C. In a previous study,<sup>12</sup> an increase of the HX4000 viscosity with time was observed, but only at 385°C and after 4 min; however, because the residence times on the extruder and injection molding equipment were less than 2 min and the working temperatures were lower than 385°C, we assumed that there was not enough time for cross-linking or other significant chemical reactions to occur. Thus, four ratios of PEEK/LCP blends (80/20, 70/30, 50/50, and 30/70) were prepared.

### Dynamic Mechanical Thermal Analysis (DMTA)

In order to confirm previous studies on miscibility,<sup>9</sup> DMT experiments were performed on the samples using a DMTA module from Polymers Lab. The scanning rate used was 2°C/min, at a frequency of 1 Hz, and strain of 4 (64 μm). The tests were done

in the bending mode, before and after annealing (230°C, 48 h).

### Differential Scanning Calorimetry (DSC)

A Perkin-Elmer DSC-7 was used to study the crystallization kinetics of the blends. The nonisothermal crystallization on heating was performed at 5, 10, and 20°C/min; on cooling from the melt (380°C, 5 min) the same absolute rates were used. The isothermal experiments were done at crystallization temperatures,  $T_c$ , of 315, 312, 310, and 307°C, from the melt (380°C, 5 min) under a nitrogen atmosphere.

### Polarized Light Optical Microscopy (PLOM)

Films for PLOM were produced by melting at 380 ± 3°C and 400 ± 5°C, in a vacuum oven, during 30 min. After melting, the films were slowly cooled (~ 40°C/h) down to 315°C; the samples remained at this temperature during 5 h. The micrographs were obtained by using a Jenaval (Carl Zeiss) microscope.

## RESULTS AND DISCUSSION

### DMTA

Table I shows the DMT data for the blends, before and after annealing. The  $T_g$  values were taken at the maximum in  $E''$  (loss modulus). Data before annealing was similar to previous studies,<sup>9</sup> in which a PEEK cold crystallization temperature (increase in  $E'$ , the storage modulus) around 164.5°C, also appears. It can also be observed that, after annealing, only one  $T_g$  appears, indicating miscibility. Resolution of the  $T_g$ s can be poor due to three factors: the  $T_g$ s of the pure components are less than 20°C

**Table I** Dynamic Mechanical Thermal Data of Blends

Composition (PEEK/HX4000)	Before Annealing			After Annealing
	$T_g$ PEEK (°C)	$T_g$ HX4000 (°C)	$T_c$ PEEK (°C)	$T_g$ (°C)
100/0	142.8 ± 0.6	—	165.5 ± 0.7	157.2 ± 0.7
80/20	140.2 ± 0.2	—	164.5 ± 0.7	156.1 ± 0.3
70/30	142.2 ± 1.7	—	164.3 ± 0.4	154.0 ± 0.3
50/50	141.5 ± 4.5	162.2 ± 1.2	164.5 ± 0.7	153.7 ± 0.3
30/70	141.8 ± 0.8	161.5 ± 0.1	—	153.5 ± 3.8
0/100	—	158.9 ± 1.6	—	159.4 ± 0.3

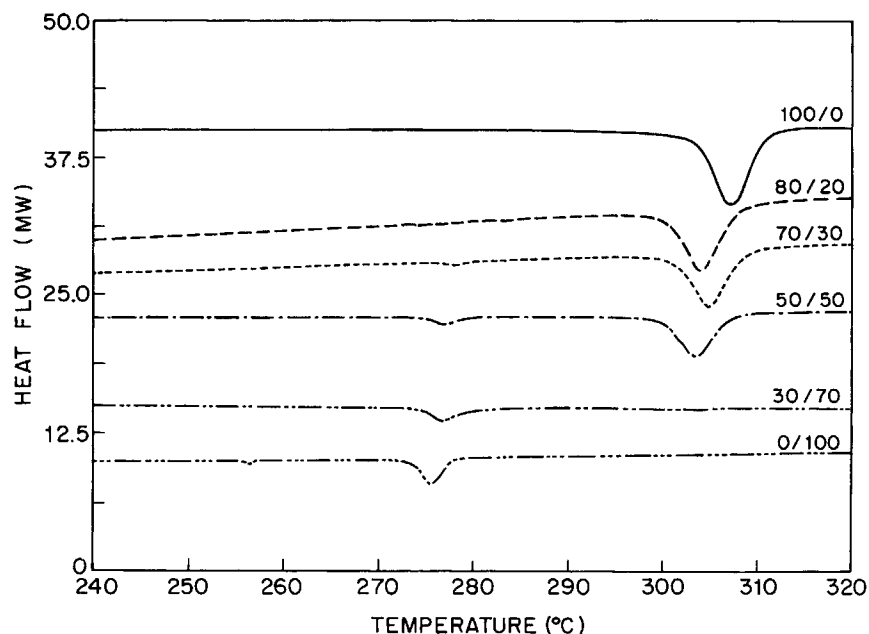


**Figure 1** Typical nonisothermal crystallization curves of the blends on cooling from the melt ( $-5^{\circ}\text{C}/\text{min}$ ).

apart from each other; the HX4000  $\tan \delta$  peak is small and broad; and cold crystallization occurs at temperatures intermediate to both  $T_g$ s. However, after annealing, besides this data, miscibility of the amorphous phases was also confirmed by scanning electron microscopy<sup>9</sup> and DMA using the torsion mode of the Rheometrics Mechanical Spectrometer 800.<sup>9</sup>

It was also observed that the  $T_g$  values, at all compositions, are lower than the  $T_g$ s of the pure components, which can be interpreted as a plasticization effect of the LCP on the PEEK.

### Nonisothermal Crystallization

Figure 1 shows typical nonisothermal crystallization curves of the blends from the melt. Two crystallization peaks can be observed: the high temperature peak corresponds to the PEEK crystallization, the low temperature peak is due to the LCP. These values ( $T_{c,c}$ ), along with the enthalpy of crystallization ( $\Delta H_{c,c}$ ) as a function of the cooling rate are shown in Table II. The addition of the LCP in general decreases the PEEK crystallization temperature and retards the beginning of the crystallization probably due to partial or total miscibility of both components in the melt stage. One study<sup>13</sup> pointed out that a phase separated component can also influence the crystallization behavior; however, we believe that if the polymers were immiscible in the melt state, the

noncrystallizable component probably would accelerate the beginning of the crystallization due to heterogeneous nucleation. This behavior has been confirmed by isothermal and nonisothermal crystallization studies of blends of PPS/HX4000.<sup>14</sup> On the other hand, the HX4000 crystallization temperature increases slightly with the increase of the amount of PEEK in the blend. The PEEK is probably acting as a nucleating agent for the LCP crystals.

The  $\Delta H_{c,c}$  values of the HX4000 are much lower than of the PEEK, as expected. This has already been observed in other studies<sup>15</sup> and has been attributed to an imperfect packing of the chains and to the low conformational alteration that occurs during the nematic-crystalline solid transition.

In all these scanings, when it appeared, only one  $T_g$  was observed.

Figure 2 shows a typical heating scan of the blends and Table III summarize this behavior as a function of the heating rate. In general, two melting peaks and a cold crystallization peak can be observed. Some authors<sup>16</sup> have found two melting endotherms, at  $\sim 225$  and  $337^{\circ}\text{C}$ , for pure PEEK, both varying with the heating rate. As the heating rate is increased, the heat of fusion of the low temperature endotherm increased and that of the high temperature endotherm decreased. However, in our studies, only the high temperature endotherm was observed. This last temperature decreases slightly with the addition of LCP; probably the LCP reduces the per-

**Table II** Values of  $T_{c,c}$  and  $\Delta H_{c,c}$  of Blends after Nonisothermal Crystallization on Cooling

PEEK/HX4000	Rate (°C/min)	$T_{c,c}$ (°C)		$-\Delta H_{c,c}$ (J/g)	
		PEEK	HX4000	PEEK	HX4000
100/0	-5	307.5 ± 0.4	—	40.0 ± 7.0	—
80/20	—	303.7 ± 0.5	276.4	45.0 ± 0.0	2.0
70/30	—	304.0 ± 1.0	277.3 ± 0.9	43.9 ± 0.3	3.3 ± 0
50/50	—	303.2 ± 0.4	276.6 ± 0.3	41.4 ± 0.0	5.0 ± 0.3
30/70	—	303.3 ± 0.6	276.2 ± 0.9	5.3 ± 2.0	8.6 ± 0.8
0/100	—	—	275.4 ± 0.1	—	8.2 ± 1
100/0	-10	301.1	—	39.7	—
80/20	—	290.0 ± 4.0	—	43.5 ± 0.8	—
70/30	—	295.0 ± 5.0	269.0 ± 4.0	45.1 ± 1.0	2.1 ± 0.4
50/50	—	299.8 ± 0.7	276.1 ± 0.3	48.6 ± 1.0	3.9 ± 0.7
30/70	—	298.9 ± 0.6	275.1 ± 0.6	5.6 ± 2.0	8.4 ± 0.3
0/100	—	—	275.0	—	7.9
100/0	-20	293.2 ± 0.3	—	41.9 ± 1.0	—
80/20	—	289.3 ± 0.1	270.1 ± 0.2	38.3 ± 0.2	1.8 ± 0.4
70/30	—	289.5 ± 0.1	270.7 ± 0.1	39.2 ± 0.1	3.3 ± 0.0
50/50	—	289.2 ± 0.5	270.2 ± 0.4	39.3 ± 0.1	5.3 ± 0.1
30/70	—	289.0 ± 0.9	269.7 ± 0.6	5.0 ± 3.0	8.2 ± 0.3
0/100	—	—	269.3 ± 0.7	—	7.5 ± 0.2

$T_{c,c}$ , crystallization temperature on cooling and  $\Delta H_{c,c}$ , enthalpy of crystallization on cooling. Standard deviations of three separate measurements are also given.

fection of the PEEK crystals. On the other hand, the LCP melting temperature increases slightly with the increase of PEEK; in this case, PEEK probably

increases the perfection of the LCP crystalline solid domains, altering its rotational and translational organization.

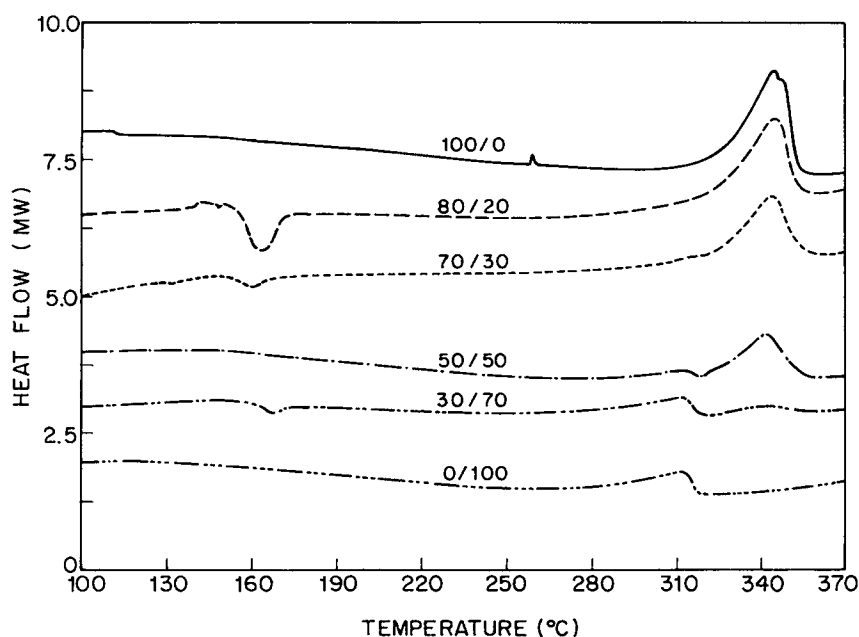


**Figure 2** Typical nonisothermal crystallization curves of the blends on heating from above room temperature (5°C/min).

**Table III** Values of  $T_{c,h}$  and  $T_{m,h}$  of Blends after Nonisothermal Crystallization on Heating

PEEK/HX4000	Rate (°C/min)	$T_{c,h}$ (°C) PEEK	$T_{m,h}$ (°C) PEEK	$T_{m,h}$ (°C) HX4000
100/0	5	—	343.4 ± 3.7	—
80/20	—	161.7 ± 1.1	343.1 ± 3.0	—
70/30	—	159.6 ± 1.7	342.0 ± 3.8	312.0 ± 2.5
50/50	—	165	341.3 ± 2.9	311.3 ± 2.0
30/70	—	166.6 ± 1.2	340.0 ± 3.3	310.3 ± 2.0
0/100	—	—	—	310.2 ± 2.0
100/0	10	167.4 ± 1.3	342.3 ± 0.3	—
80/20	—	165.0 ± 1.0	340.6 ± 2.4	—
70/30	—	164.6 ± 1.0	339.8 ± 2.5	310.4 ± 2.3
50/50	—	169.2 ± 2.0	339.6 ± 1.0	311.1 ± 0.2
30/70	—	169.7 ± 1.9	337.4 ± 0.7	307.1 ± 0.6
0/100	—	—	—	307.4 ± 0.6
100/0	20	141.2 ± 3.0	346.2 ± 4.0	—
80/20	—	146.2 ± 167.8	343.6 ± 4.0	—
70/30	—	166.7 ± 3.4	340.9 ± 1.7	311.0 ± 0.8
50/50	—	171.2 ± 2.4	339.8 ± 1.8	310.9 ± 0.1
30/70	—	176.7 ± 1.4	337.8 ± 3.0	308.8 ± 3.0
0/100	—	—	—	309.6 ± 2.7

$T_{c,h}$ , crystallization temperature on heating and  $T_{m,h}$ , melting temperature on heating. Standard deviation of three separate measurements are also given.

### Isothermal Crystallization

#### Avrami Analysis

Figure 3 shows a typical isothermal crystallization scan of the blends at 315°C. From these curves,  $X_c(t)$

and  $X_c(\infty)$  can be calculated and a plot of  $\{-\ln[1 - X_c(t)/X_c(\infty)]\}$  as a function of time can be drawn. Figure 4 shows a typical Avrami plot of the blends (315°C). It can be observed that the curves present two regions: one linear followed by a roll-off at longer times, each region giving a different value for  $n$  ( $n_1$

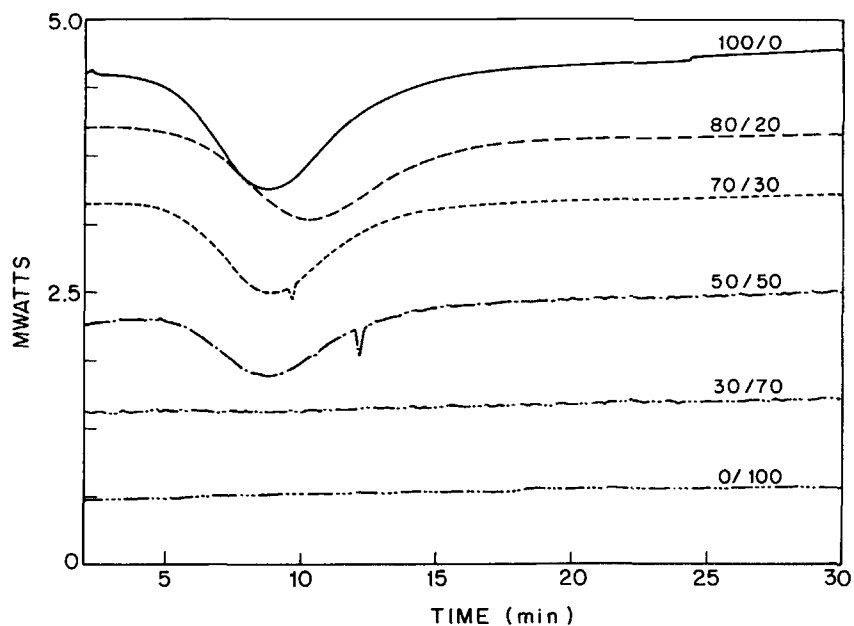


**Figure 3** Typical DSC isothermal crystallization curves of the blends (315°C).

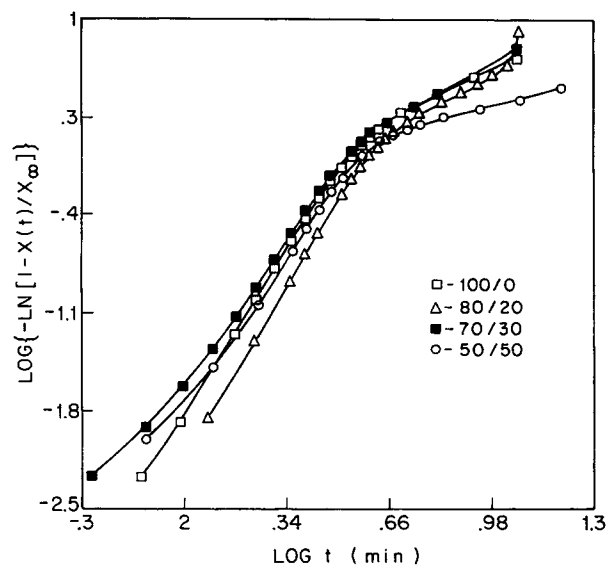


Figure 4 Typical Avrami plot of the blends (315°C).

and  $n_2$ ) and  $k$  ( $k_1$  and  $k_2$ ). Two different values of  $n$  can represent two different crystallization mechanisms, the second one due to secondary crystallization or crystal perfection. This data is shown in Table IV.

The PEEK  $n_1$  values (3.5–3.8) can be interpreted as representative of spherulitic growth from spo-

radically formed nuclei.<sup>17</sup> It can be pointed out that  $n_1$  can also change with the holding time in the melt, as observed in a recent study,<sup>10</sup> where PEEK was melted at 380°C for 2 min and  $n_1$  was found to vary between 2.0 and 2.4. A previous study<sup>16</sup> relates this difference to the high viscosity and chain entanglements that occur in the melt, because it may take a long time for the crystalline regions in the bulk to lose order and become a completely homogeneous melt. In the blends, except composition 30/70, the  $n_1$  values vary between 3.3 and 3.9, indicating that the crystallization morphology is the same as in pure PEEK.

Avrami analysis of the “roll-over” portion of the curves is not appropriate because secondary crystallization is not treated in the Avrami approach.

Figure 5 shows  $k_1$  of the blends as a function of crystallization temperature. It can be observed that  $k_1$  (or the overall crystallization rate) decreases with temperature, as expected. The overall crystallization rates of pure PEEK, at all crystallization temperatures, are higher than of the blends. However, a small amount of LCP (20 wt %) added to this polymer decreases its crystallization rate more strongly than a higher amount (50 or 70 wt %). It seems that 20 wt % of LCP in the PEEK acts as a more effective diluent (or plasticizer, as already reported<sup>12</sup>) than higher amounts.

Table IV  $n$  and  $k$  ( $\text{min}^{-n}$ ) Avrami Parameters of Blends as Function of Crystallization Temperature

Composition (PEEK/HX4000)	Crystallization Temperature	$n_1$	$k_1$	$n_2$	$k_2$
100/0	315°C	3.5	$2.9 \times 10^{-3}$	1.4	$1.0 \times 10^{-1}$
80/20		3.4	$6.8 \times 10^{-4}$	1.3	$8.2 \times 10^{-2}$
70/30		3.8	$8.6 \times 10^{-4}$	1.4	$1.6 \times 10^{-1}$
50/50		3.5	$1.6 \times 10^{-3}$	2.2	$2.9 \times 10^{-2}$
30/70		—	—	—	—
100/0	312°C	3.7	$1.1 \times 10^{-2}$	1.9	$1.8 \times 10^{-1}$
80/20		3.7	$3.1 \times 10^{-3}$	1.4	$1.6 \times 10^{-1}$
70/30		3.5	$5.6 \times 10^{-3}$	1.5	$1.6 \times 10^{-1}$
50/50		3.3	$1.5 \times 10^{-2}$	1.9	$1.6 \times 10^{-1}$
30/70		—	—	—	—
100/0	310°C	3.7	$3.2 \times 10^{-2}$	1.3	$4.0 \times 10^{-1}$
80/20		3.9	$6.3 \times 10^{-3}$	1.5	$1.9 \times 10^{-1}$
70/30		3.6	$1.4 \times 10^{-2}$	0.9	$4.9 \times 10^{-1}$
50/50		3.5	$1.2 \times 10^{-2}$	0.9	$5.1 \times 10^{-1}$
30/70		2.7	$4.9 \times 10^{-2}$	1.0	$2.9 \times 10^{-1}$
100/0	307°C	3.8	$1.3 \times 10^{-1}$	1.1	$7.3 \times 10^{-1}$
80/20		3.7	$3.2 \times 10^{-2}$	0.7	$9.3 \times 10^{-1}$
70/30		3.9	$2.7 \times 10^{-2}$	0.7	$7.5 \times 10^{-1}$
50/50		3.7	$4.0 \times 10^{-2}$	1.1	$6.7 \times 10^{-1}$
30/70		2.8	$9.0 \times 10^{-2}$	1.1	$4.5 \times 10^{-1}$

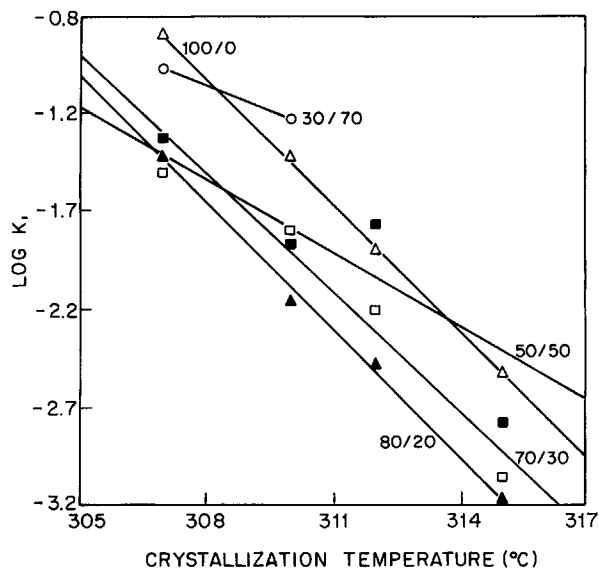


**Figure 5**  $k_1$  of the blends as a function of crystallization temperature.

Data of the time necessary for maximum crystallization to occur,  $t_{max}$ , is shown in Figure 6. This time corresponds to the point where  $dQ/dt = 0$ ,  $Q(t)$  being the heat flow rate. It can be seen that the 80/20 blend presents the highest  $t_{max}$ , confirming that, at this composition, the LCP acts as a more effective diluent, retarding the PEEK crystallization in the blend.

The induction times,  $t_i$ , as a function of composition are shown in Figure 7. It is observed that  $t_i$  decreases as the crystallization temperature decreases, as expected. At 315 and 312°C,  $t_i$  increases

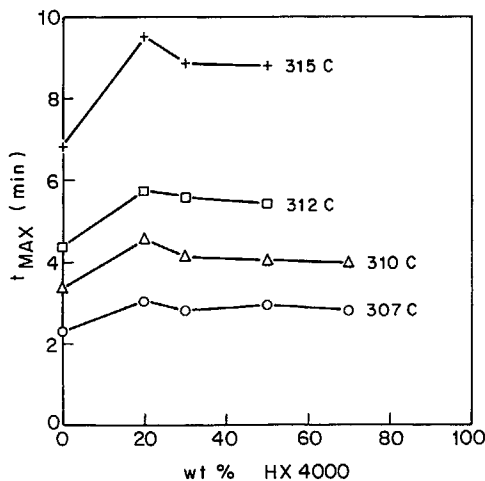


**Figure 6**  $t_{max}$  of the blends as a function of composition and crystallization temperature.

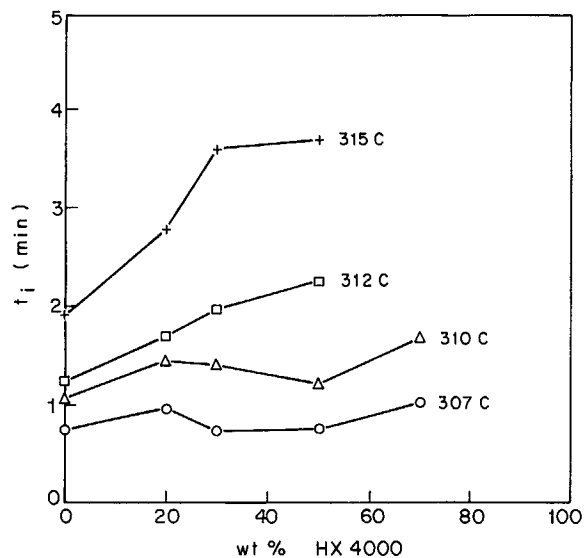


**Figure 7**  $t_i$  of the blends as a function of composition and crystallization temperature.

with the amount of LCP. However, at 310 and 307°C the behavior of the curves changes, showing a maximum at the 80/20 composition. The LCP melts around 307–310°C. Thus, the PEEK crystallization kinetics will be different below 310°C because the LCP is changing from a solid crystalline to a nematic mesophase. This observation needs further studies.

**Hoffmann et al. Analysis**

Figure 8 shows a graph where the left-hand term of eq. (6), A, has been plotted as a function of  $1/T\Delta T$  ( $\varphi$ ). To calculate this expression the following pa-

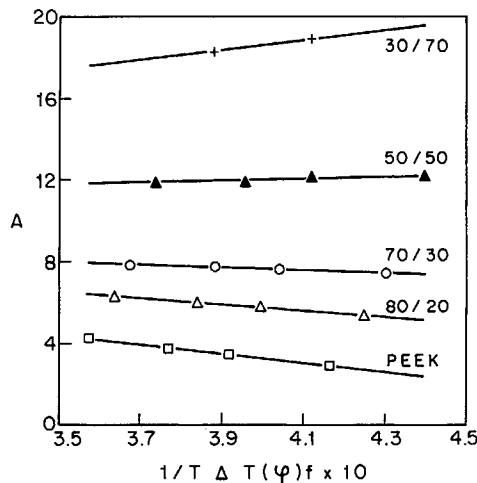


**Figure 8** Left-hand term of eq. (6) as a function of  $1/T\Delta T$  of the blends.



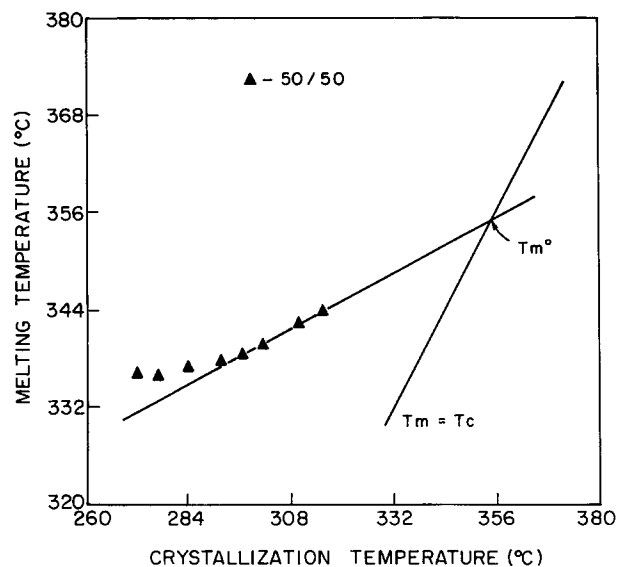


Figure 9 Typical plot for calculation of  $T_m^0$  and  $\alpha$  of the blends.

rameters were used<sup>7-11</sup>:  $U^* = 8.38$  kJ/mol;  $C_2 = 51.6^\circ\text{C}$ ;  $b_0 = 0.2929$  nm;  $\beta = 0.24$ ;  $\Delta H_m^0 = 130$  J/g;  $\rho_{\text{PEEK}} = 1.263$  g/cm<sup>3</sup>,  $\rho_{\text{HX4000}} = 1.287$  g/cm<sup>3</sup>.

$\beta$  was considered to be equal to 0.24, because as already pointed out by some authors,<sup>8</sup> "the presence of oxygen atoms on the lateral surfaces suggests that  $\beta$  for PEEK might be similar to that of polyesters."

The values of  $k_1$  and  $n_1$  are given in Table IV.

The values of  $T_m^0$  were calculated by using the following eq.<sup>4</sup>:

$$T_m = T_m^0 (1 - 1/2\alpha) + T_c/2\alpha \quad (8)$$

where  $\alpha$  = lamellar thickening factor (the final lamellar thickness will be  $\alpha$  times larger than the initial thickness).

A typical Hoffmann and Weeks plot of  $T_m$  vs.  $T_c$  is shown in Figure 9. The deviation from a straight line of some of the data points can be caused by recrystallization or reorganization,<sup>18,19</sup> that usually

Table V Extrapolated ( $T_m^0$ ) Values of Blends

Composition (PEEK/HX4000)	$T_m^0$ (°C)	$\alpha$
100/0	357.3	1.52
80/20	356.4	—
70/30	355.9	—
50/50	355.0	1.81
30/70	353.2	1.85

Table VI. Fold Surface Free Energy,  $\sigma_e$ , as Function of Composition

Composition (PEEK/HX4000)	$\sigma_e$ (erg/cm <sup>2</sup> )	Correlation Coefficient
100/0	$37 \pm 5$	-0.999
80/20	$25 \pm 4$	-0.993
70/30	$14 \pm 4$	-0.981
50/50	$-8 \pm 4$	0.81
30/70	$-41 \pm 9$	—

occurs at low  $T_c$  values during the thermal analysis experiment. As a consequence, the  $T_m$  values obtained for high  $T_c$  values are apt to be more correct than those obtained for low  $T_c$  values.  $T_m^0$  is the intercept of the extrapolated  $T_m$  values and the line  $T_m = T_c$ . The  $T_m^0$  and  $\alpha$  values are given in Table V. A slight depression of the equilibrium melting point was observed, indicating miscibility of both components, and as expected,<sup>4</sup> the final lamellar thickness of the PEEK crystals in the blends was larger than in the pure state due to a decreased supercooling. It is also known<sup>19</sup> that large  $\alpha$  values can indicate that recrystallization has occurred.

The values of  $T_g$ s are given in Table I;  $\sigma$  was calculated from eq. (7), being equal to 19 erg/cm<sup>2</sup>.

The values of  $\sigma_e$  were calculated from the slopes of the curves of Figure 8, assuming a regime III of crystallization kinetics<sup>8</sup> and are shown in Table VI. The  $\sigma_e$  value of pure PEEK ( $37 \pm 5$  erg/cm<sup>2</sup>) is similar to the ones found in the literature.<sup>6,8</sup> However, in our case, this value decreases with the increase of LCP, even being negative at low concentrations of PEEK. It can also be observed that the correlation coefficient is close to 1 up to a 70/30 composition; however above this composition, this correlation coefficient decreases indicating an imperfect correlation. The 30/70 system did not present crystallization at 312 and 315°C, and only two points could be used to plot the data. The decrease of  $\sigma_e$  has been

Table VII Lateral Surface Free Energy,  $\sigma$ , for  $\sigma_e = 37$  erg/cm<sup>2</sup>

Composition (PEEK/HX4000)	$\sigma$ (erg/cm <sup>2</sup> )
100/0	19.0
80/20	15.6
70/30	10.0
50/50	7.5
30/70	5.2

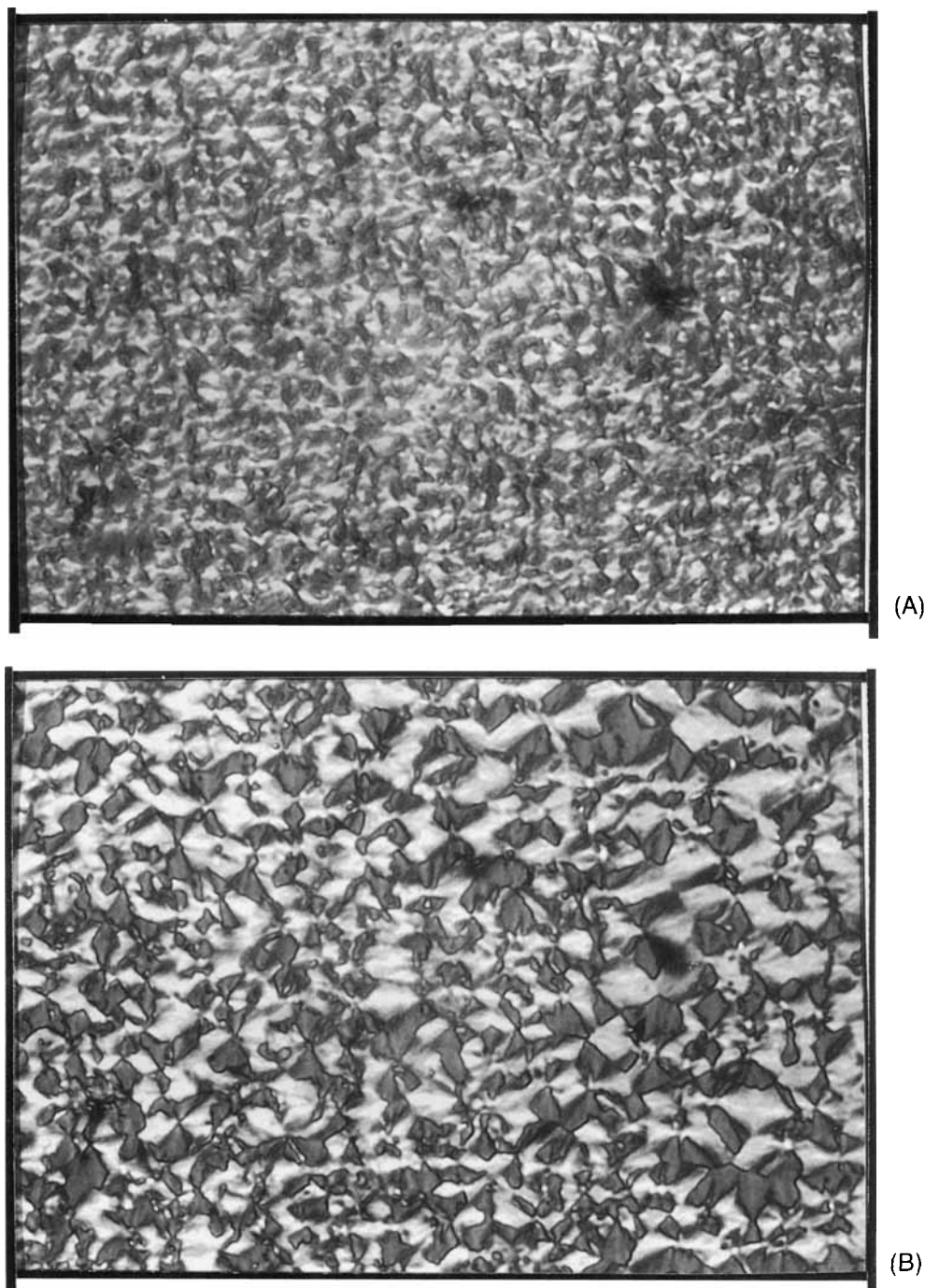


**Figure 10** (a) PEEK isothermally crystallized at 315°C after melting at 380°C (magnification 1000×); (b) PEEK isothermally crystallized at 315°C after melting at 400°C (magnification 1000×).

observed<sup>7</sup> when a nucleating agent is added to an iPP/dotriacontane mixture. This lowering is explained<sup>7</sup> as a consequence of the occurrence of multiple nucleation, which leads to the formation of loops and tie molecules and dangling chain ends

from cilia. Also, comparing two different poly(aryl ether ketones),<sup>6</sup> it was found that the product  $\sigma\sigma_e$  was higher for PEEK than for polyetherketoneketone (PEKK); the discrepancy was explained as due to the chemical structure of the PEKK that might

facilitate the chain folding mechanism, and consequently lower the crystal-surface free energy.

If we assume that eq. (6) is valid for our system and that the PEEK parameters are experimentally correct, then two factors can be considered responsible for these "anomalous" values of  $\sigma_e$ : the value of  $\sigma$  is not constant or the kinetic regime is not regime III, as assumed. In this last case, if a transition to regime II occurs,  $r$  would have to be equal to 2,  $\sigma_e$  would double, but still would decrease and would be negative. Regarding  $\sigma$ , it has been observed that almost all the literature on blends assume that in the case of PEEK,  $\sigma$  is equal to 19 erg/cm<sup>2</sup> and it is constant at all blend compositions. This last assumption is valid when the diluent is a noncrystallizable polymer that will also be a random coil in the melt state as the PEEK is. Thus  $\sigma$  will not be affected for the presence of other macromolecules with the same melt characteristics as that of the PEEK. However, the LCP is a rigid macromolecule that will not be a random coil in the melt state; its conformation will be more similar to the lateral surface of the PEEK crystallizing macromolecule. Thus, the LCP can affect the value of  $\sigma$  in the blend. To confirm this last hypothesis, we calculated the values of  $\sigma$  that would result if we took  $\sigma_e$  constant and equal to 37 erg/cm<sup>2</sup>. The values are shown in Table VII. It can be observed that if  $\sigma_e$  is constant at all compositions,  $\sigma$  will decrease, but will be positive. In other words, the LCP rigid chains diminish the amount of lateral surface free energy that the PEEK macromolecules will expend to crystallize; this increased reduction in  $\sigma$  can eventually increase the thickness of the lamellae producing more extended PEEK crystals, as inferred from the calculated  $\alpha$  values. As a matter of fact, we believe that in our systems neither  $\sigma$  nor  $\sigma_e$  can be considered constants; both probably change with composition.

## PLOM

Two melting temperatures (380 and 400°C) were used because results of a recent study<sup>10</sup> showed that the PEEK spherulitic morphology was dependent on the melting temperature.

Figure 10 shows this difference; at 380°C [Fig. 10(a)], no spherulites (or very small spherulites) can be observed; at 400°C [Fig. 10(b)] a coarse texture and a spherulitic morphology is seen. Probably, at 380°C the PEEK did not melt completely and self-nucleation occurred, and at 400°C, it melted completely and heterogeneous nucleation happened.

Micrographs of the blends are also shown in Figure 11; the blend 80/20 has the same spherulitic

morphology as pure PEEK, whatever the melting temperature [Fig. 11(a)]. This result confirms the Avrami analysis. However, the other compositions do not present this spherulitic morphology at any melting temperature [Fig. 11(b-d)]. Instead, a droplet and fibrillar-like morphology is observed. The HX4000 [Fig. 11(e)] showed a typical Schlieren texture, probably nematic. The "dark brushes" correspond to the extinction positions of the mesophases.<sup>20</sup> Evidently, this last micrograph shows the LCP in its solid crystalline form, because the nematic-solid transition of this polymer occurs around 270°C.

## CONCLUSIONS

The nonisothermal crystallization experiments from the melt showed that the LCP retards the PEEK crystallization process, probably due to miscibility of both components in the melt state. The experiments on heating revealed that the PEEK melting temperature decreased with the amount of LCP, and on the other hand, the LCP melting temperature increased with the amount of PEEK. Thus, the PEEK probably improves the perfection of the LCP crystalline domains, while the LCP do not. The increase of an LCP melting temperature with annealing<sup>21</sup> has been attributed to "an ester interchange reorganization which induces the conversion of a random to block copolymer." In our case, probably two main factors contributed to increasing the HX4000 melting temperature: the annealing promoted by the DSC itself and the presence of the PEEK. Thus, this topic needs further research.

The isothermal crystallization Avrami analysis showed that a spherulitic morphology in pure PEEK and its blends with LCP should be expected, independent of the crystallization temperature. However, this spherulitic morphology was observed by PLOM only for pure PEEK and for the 80/20 composition. The other compositions presented a droplet and fibrillar-like morphology.

The overall crystallization rate was observed to decrease with the crystallization temperature for all compositions. There are two factors that can influence the PEEK crystallization: there is the effect promoted by the dilution of the PEEK, that will retard the crystal growth changing the crystallization peak to higher times and also the "plasticization" (or reduction of viscosity) of the PEEK promoted by the HX4000.<sup>12</sup> Thus the behavior of the crystallization peak with concentration will depend on the balance between these two factors.

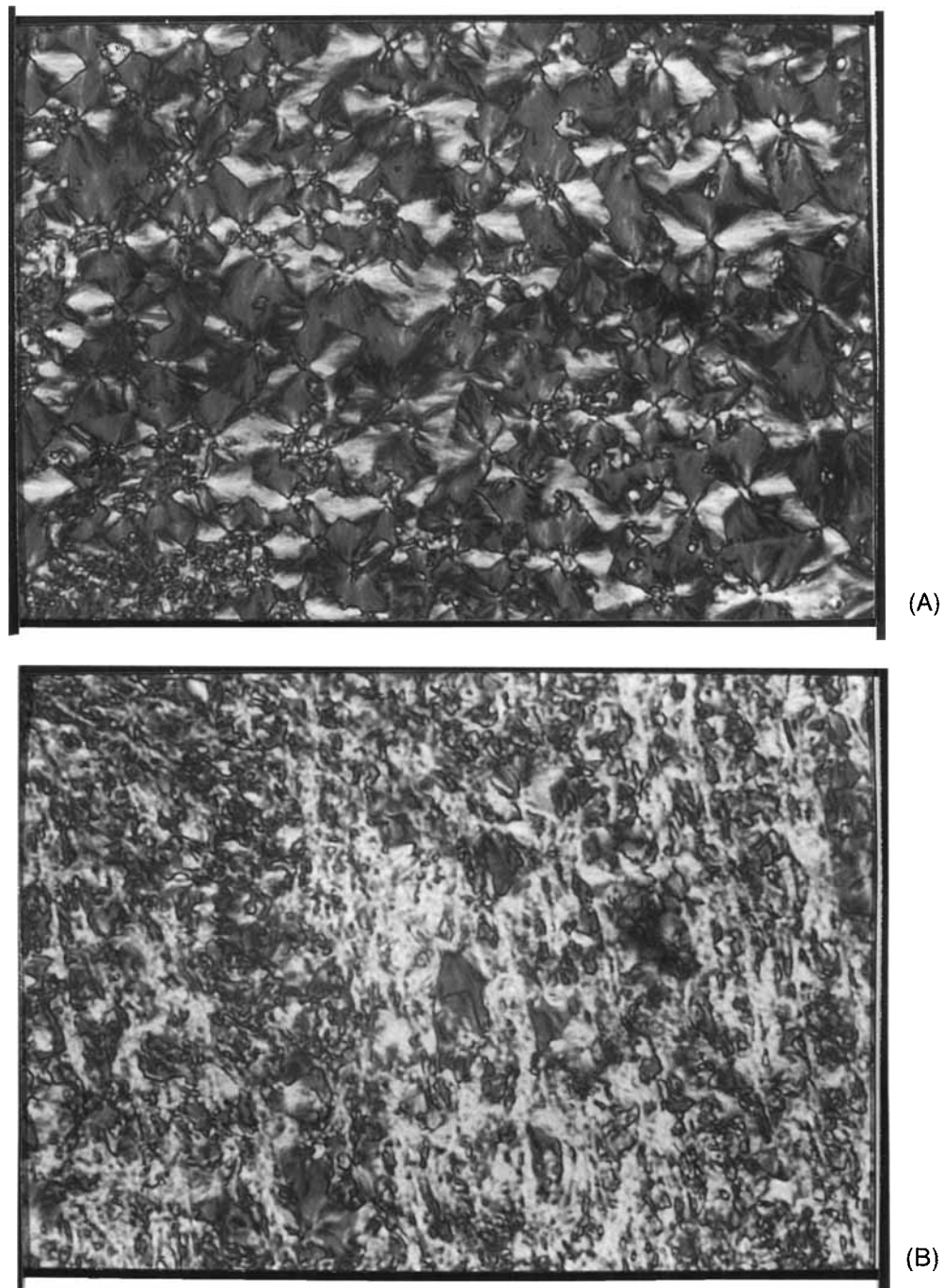
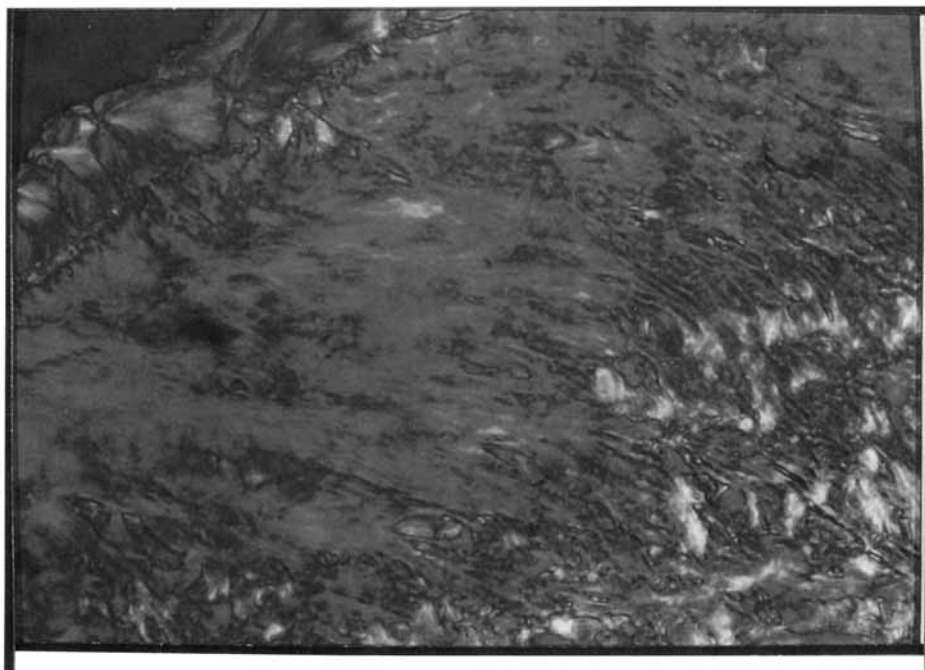
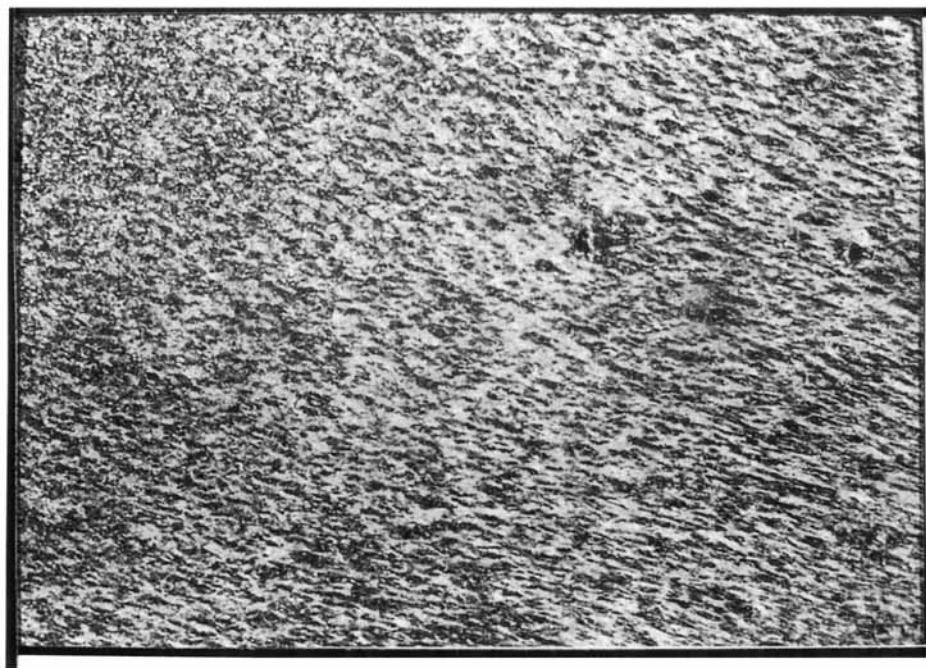


**Figure 11** (a) 80/20 blend isothermally crystallized at 315°C after melting at 400°C (magnification 1000×); (b) 70/30 blend isothermally crystallized at 315°C after melting at 400°C (magnification 1000×); (c) 50/50 blend isothermally crystallized at 315°C after melting at 400°C (magnification 1000×); (d) 30/70 blend isothermally crystallized at 315°C after melting at 400°C (magnification 1000×); (e) HX4000 isothermally crystallized at 315°C after melting at 400°C (magnification 1000×).



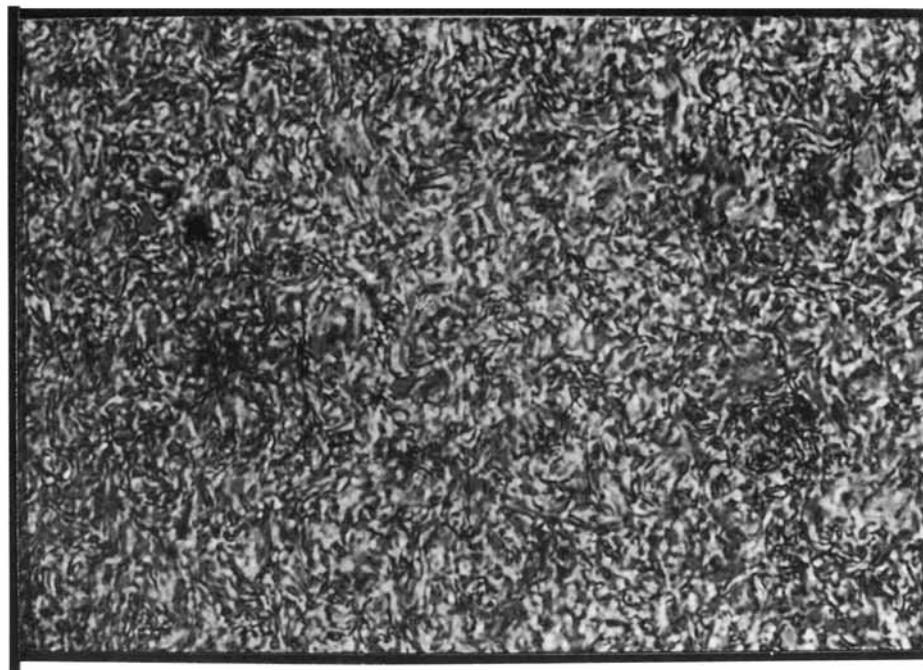
(C)



(D)

The value of  $\sigma_e$  for pure PEEK was found to be equal to  $37 \pm 5 \text{ erg/cm}^2$ , similar to previous studies. However, it was observed that  $\sigma_e$  decreased with the increase in the amount of LCP, having unrealistic negative values. This discrepancy was attributed to the value of  $\sigma$  that in the calculations was maintained constant. Thus, it was observed that if we

assumed that  $\sigma_e$  was constant, instead of  $\sigma$ , this last one would decrease, but still remained positive. Physically, this would mean that the presence of LCP rigid chains lowered the lateral surface free energy that the PEEK macromolecules would expend on crystallization, resulting in more extended crystals. As a matter of fact, we concluded that nei-



(E)

Figure 11 (Continued from the previous page)

ther  $\sigma$  nor  $\sigma_e$  can be considered constant for these blends. These last observations need further studies to be corroborated.

The authors wish to express their gratitude to FAPESP (92/0990-2) for the financial support and to Dr. Donald G. Baird for the preparation of the samples.

## REFERENCES

1. J. D. Hoffmann, *Polymer*, **23**, 656 (1982).
2. J. D. Hoffmann and R. L. Miller, *Macromolecules*, **21**, 3038 (1988).
3. J. D. Hoffmann, G. T. Davis, and J. I. Lauritzen, Jr., *Treatise on Solid State Chemistry*, Vol. 3, N. B. Hannay, Ed., Plenum Press, New York, 1976, Chap. 7.
4. J. P. Runt and L. M. Martynowicz, *Multicomponent Polymer Materials, Advances in Chemistry Series*, D. R. Paul and L. H. Sperling, Eds., 1986, Chap. 7.
5. T. T. Wang and T. Nishi, *Macromolecules*, **10**, 421 (1977).
6. B. S. Hsiao and B. B. Sauer, *J. Polym. Sci. B, Polym. Phys.*, **31**, 901 (1993).
7. G. B. A. Lim and D. R. Lloyd, *Polym. Eng. Sci.*, **33**, 513 (1993).
8. G. C. Alfonso, V. Chiappa, J. Liu, and E. R. Sadiku, *Eur. Polym. J.*, **27**, 795 (1991).
9. R. E. S. Bretas and D. G. Baird, *Polymer*, **33**, 5233 (1992).
10. A. Morales and R. E. S. Bretas, *Polymer*, to appear.
11. P. Cebe and S. Hong, *Polymer*, **27**, 1183 (1986).
12. R. E. S. Bretas, D. Collias, and D. G. Baird, *Polym. Eng. Sci.*, to appear.
13. E. Martuscelli, *Polym. Eng. Sci.*, **24**, 563 (1984).
14. G. Gabellini and R. E. S. Bretas, unpublished data.
15. S. Z. D. Cheng, *Macromolecules*, **21**, 2475 (1988).
16. Y. Lee and R. S. Porter, *Macromolecules*, **21**, 2770 (1988).
17. B. Wunderlich, *Macromolecular Physics*, Vol. 2, Academic Press, New York, 1976.
18. J. P. Runt and K. P. Gallagher, *Polym. Commun.*, **32**, 180 (1991).
19. J. D. Hoffmann and J. J. Weeks, *J. Res. A, Phys. Chem.*, **66A**, 1, 13 (1962).
20. L. H. Sperling, *Introduction to Physical Polymer Science*, 2nd ed., John Wiley & Sons, Inc., New York, 1992.
21. A. M. Ghanem, L. C. Dickinson, and R. S. Porter, *J. Polym. Sci. B, Polym. Phys.*, **28**, 1891 (1990).

Received March 25, 1994

Accepted July 6, 1994